Study of the XANES Modeling of Molybdenum Compounds

John Evans* and J. Frederick W. Mosselmans

Contribution from the Department of Chemistry, The University, Southampton, England SO9 5NH. *Received July 17, 1990*

Abstract: The structural factors affecting the Mo K-edge XANES features for series of mono- and dimeric complexes have been investigated by using the one-electron multiple scattering approach of the program DLXANES utilizing ab initio phase shifts calculated from atomic charge densities. The main aspects of the experimental spectra could be reproduced, with the following generalizations. (1) Low Z backscatterers were more important contributors to the near-edge pattern (as in $Li_4[Mo_2(Me)_8]\cdot 4Et_2O$). (2) Bond length variations of ca. 0.2 Å could be identified solely in the XANES region. (3) Intrashell multiple scattering pathways allowed the differentiation of coordination centers with differing bond angles at molybdenum, e.g. tetrahedral versus square planar or trigonal-bipyramidal versus square pyramidal. (4) Some evidence could be found for contributions from shells not identifiable in the EXAFS region of the spectrum (e.g. the Mo--Li shell at 2.74 Å in $Li_4[Mo_2(CH_3)_8]\cdot 4Et_2O$).

Introduction

The extent of the near-edge region is the subject of some discussion but here it is considered to be the 30 eV before the edge and up to 70 eV past it. Benfatto et al.[1] have claimed to see the effects of multiple scattering of a type normally confined to the XANES region 160 eV past the absorption threshold in the Mn K-edge spectra of the permanganate ion and have introduced the concept of two regions, the first from 0 to 30 eV past the edge where full multiple scattering occurs and the other from 30 to 160 eV where intermediate multiple scattering is claimed to occur.

There are phenomena seen in the XANES region which are not normally observed in the EXAFS region. There are sharp peaks below the edge and in the white line region due to electronic transitions between bound states. For molybdenum K-edge spectra the principal transition seen is the 1s-5p/4d transition. This is much stronger in compounds where molybdenum is tetrahedrally coordinated and all those lacking a center of symmetry than those where it is octahedrally coordinated, where the transition is dipole-forbidden. Furthermore near the edge many-body effects may be seen.

However apart from single scattering the main contribution to the postedge XANES region comes from multiple scattering of the ejected photoelectron. There are two different types of multiple scattering to consider. Type I, intershell, whose effects are also seen in the EXAFS region, e.g. in the absorption spectra of metal carbonyls, involves linear or near-linear groups of atoms, as its influence is strongly dependent on the angle between the atoms. For linear groups the photoelectron is strongly forward scattered by the first scatterer toward the second. Type II is intrashell multiple scattering and involves scattering between atoms in the same shell in a circular path to the central atom. This type of multiple scattering offers the possibility of obtaining additional information to that available from EXAFS. Stern and Bunker[2] claimed that type II scattering is only relevant to the first 12 or 13 eV past the edge in the majority of absorption spectra and hence that the XANES region really only consists of the pre-edge and this near-XANES region.

XANES has been used as a complementary technique to EXAFS analysis for several biological systems,[3] gases,[4] and transition-metal complexes.[5] In many areas such as heterogeneous catalysis this technique has received little attention except as a basis comparative tool.[6] The theoretical and experimental states of XANES were reviewed by Durham[7] and Bianconi.[8]

There are few examples of using calculated spectra in structural analysis.[9] This is in spite of the wide availability of a program (DLXANES[10,11]) that calculates XANES spectra from phase shifts and structural parameters. The program uses a one-electron multiple scattering approach to simulate XANES spectra. The cluster is divided into shells of atoms. These have their scattering properties described by a set of phase shifts. The multiple scattering equations are solved for each shell separately, before the multiple scattering between the shells in the cluster is calculated. The scattering matrices are reduced in size by the use of any symmetries in the cluster. Combining the reflection matrix with an atomic matrix element, which links the core and excited electron states, leads to the XANES cross section in one-electron theory. Many-body effects which reduce the lifetime of the core hole and excited electron are included by means of a complex potential. This has the effect of broadening spectral features.

This approach has been used with reasonable success on a variety of structures,[12] though it is better at predicting the position of peaks rather than their relative intensities and tends to overestimate the effect of multiple scattering.[13]

This work describes calculations made with the program DLXANES to simulate the XANES spectra of a number of molybdenum compounds and the spectra of structural distortions of

(1) Benfatto, M.; Natoli, C. R.; Bianconi, A.; Garcia, J.; Marcelli, A.; Fanfoni, M.; Davoli, I. *Phys. Rev. B* **1986**, *34*, 5774.
(2) Bunker, G.; Stern, E. A. *Phys. Rev. Lett.* **1984**, *52*, 1990.
(3) Conradson, S. D.; Burgess, B. K.; Newton, W. E.; Hodgson, K. O.; McDonald, J. W.; Rubinson, J. F.; Gheller, S. F.; Mortenson, L. E.; Adams, M. W. W.; Mascharak, P. K.; Armstrong, W. A.; Holm, R. H. *J. Am. Chem. Soc.* **1985**, *107*, 7935. Hedman, B.; Frank, P.; Gheller, S. F.; Roe, A. L.; Newton, W. E.; Hodgson, K. O. *J. Am. Chem. Soc.* **1988**, *110*, 3798. Belli, M.; Scafati, A.; Bianconi, A.; Mobilio, S.; Palladino, L.; Reale, A.; Burattini, E. *Solid State Commun.* **1980**, *35*, 355. Scott, R. A. *Physica B* **1989**, *158*, 84.
(4) Bianconi, A.; Petersen, H.; Brown, F. C.; Bachrach, R. Z. *Phys. Rev. A* **1979**, *17*, 1907. Bouldin, C. E.; Bunker, G.; McKeown, D. A.; Forman, R. A.; Ritter, J. J. *Phys. Rev. B* **1988**, *38*, 10816.
(5) Wong, J.; Lytle, F. W.; Messmer, R. P.; Maylotte, D. H. *Phys. Rev. B* **1984**, *30*, 5596. Binsted, N.; Cook, S. J.; Evans, J.; Greaves, G. N.; Price, R. J. *J. Am. Chem. Soc.* **1987**, *109*, 3669. Budnick, J. I.; Tan, Z., Pease, D. M. *Physica B* **1989**, *158*, 31.
(6) Resasco, D. E.; Weber, R. S.; Sakellson, S.; McMillan, M.; Haller, G. L. *J. Phys. Chem.* **1988**, *92*, 189. Nomura, M.; Kazusaka, A.; Kakuta, N.; Ukisu, Y.; Miyahara, K. *J. Chem. Soc., Faraday Trans. I* **1987**, *83*, 1227. Clozza, A.; Bianconi, A.; Garcia, J.; Corma, A.; Burratini, E. *Physica B* **1989**, *158*, 164.
(7) Durham, P. J. In *X-ray Absorption*; Koningsberger, D. C., Prins, R., Eds.; Wiley-Interscience: New York, 1988; pp 53-82.
(8) Bianconi, A. In *X-ray Absorption*; Koningsberger, D. C., Prins, R. Eds.; Wiley-Interscience: New York, 1988; pp 573-662.
(9) Onori, G.; Santucci, A.; Della Longa, S.; Bianconi, A.; Palladino, L. *Chem. Phys. Lett.* **1988**, *149*, 289. Kutzler, F. W.; Hodgson, K. O.; Donlach, S. *Phys. Rev. A* **1982**, *26*, 3020. Kutzler, F. W.; Natoli, C. R.; Misemer, D. K.; Doniach, S.; Hodgson, K. O. *J. Chem. Phys.* **1984**, *73*, 3274. Fujikawa, T.; Okazawa, T.; Yamasaki, K.; Tang, J.-C.; Murata, T. *Physica B* **1989**, *158*, 365. Strange, R. W.; Alagna, L.; Durham, P.; Hasnain, S. S. *J. Am. Chem. Soc.* **1990**, *112*, 4265.
(10) Durham, P. J.; Pendry, J. B.; Hodges, C. H. *Comput. Phys. Commun.* **1982**, *25*, 193.
(11) Durham, P. J.; Pendry, J. B.; Hodges, C. H. *Solid State Commun.* **1981**, *38*, 159.
(12) Garcia, J.; Bianconi, A.; Benfatto, M.; Natoli, C. R. *J. Physique* **1986**, *47*, C8-49. Kizler, P.; Lamparter, P.; Steed, S. *Physica B* **1989**, *158*, 392, 411.
(13) Bouldin, C. E.; Bunker, G.; McKeown, D. A.; Forman, R. A.; Ritter, J. J. *Phys. Rev. B* **1988**, *38*, 10816.

0002-7863/91/1513-3737$02.50/0

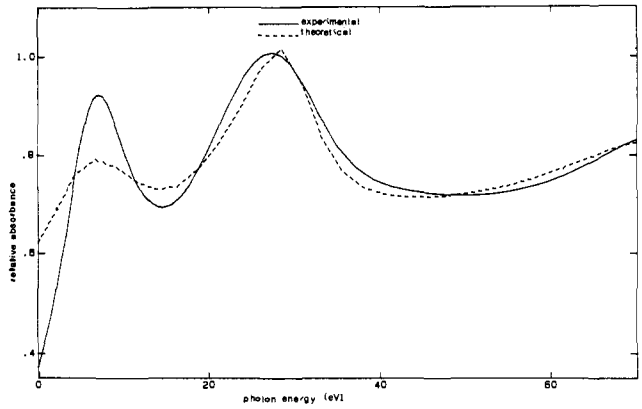

Figure 1. Experimental and theoretical XANES of $Mo(CO)_6$.

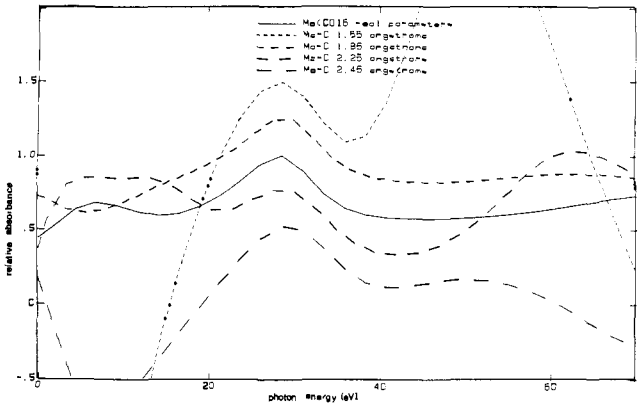

Figure 2. Theoretical XANES of $Mo(CO)_6$ showing the effect of altering the Mo–C distance.

those compounds. These studies were made to assess the current state of simple theoretical XANES modeling in order to ascertain what additional information, that was not available from conventional EXAFS analysis, could be obtained from the near-edge region. The cross section of compounds includes examples with light and heavy backscattering elements and complexes with strong to zero intershell multiple scattering.

Results and Discussion

Molybdenum Carbonyls. XANES spectra were produced by variations of the $Mo(CO)_6$ unit and the theoretical molecules $Mo(CO)_5$ and $Mo(CO)_4$. Spectra have been calculated for two basic classes of alterations to the structure. First the effect of changing either or both of the Mo–C and C–O distances was studied while maintaining an octahedral configuration. Then the number of carbonyl groups was varied and the spectra of some possible geometrical isomers were examined.

The spectrum calculated with two shells at the correct crystallographically determined distances[14] (Mo–C 2.06 Å, Mo–O 3.18 Å) is very similar to the experimental spectrum (Figure 1). These carbonyl spectra have been aligned on the second peak as the first peak in the spectra of some of the theoretical molecules is not well-defined, but all the other spectra except for those of the octacyanomolybdate ion have been aligned on the first maximum. The relative intensity of the first peak in the calculated spectrum is too small but the alignment of the peaks is good. The separation of the first two maxima is slightly smaller in the theoretical spectrum while that of the second and third peaks is larger in the calculated curve than the experimental one.

The effect of changing the Mo–C distance while the Mo–O distance is held constant is illustrated in Figure 2. This change does not affect the total pathlength of many of the Type I multiple scattering paths. Increasing either the Mo–C or the C–O distance generally results in a lengthening of the separation of the first

(14) Mak, T. C. W. *Z. Krystallogr.* **1984**, *166*, 277.

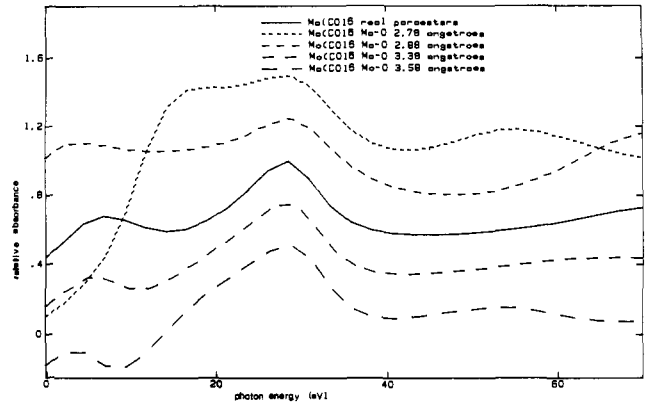

Figure 3. Theoretical XANES of $Mo(CO)_6$ showing the effect of altering the Mo–O distance.

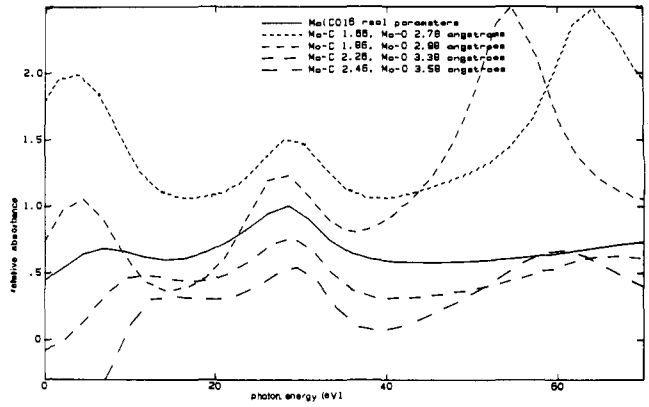

Figure 4. Theoretical XANES of $Mo(CO)_6$ showing the effect of altering the Mo–C and Mo–O distances simultaneously.

two maxima while the second and third ones become closer together. The effect on the relative intensity of the three peaks is pronounced.

Figure 3 shows the result of altering the C–O distance with the Mo–C distance held constant. The spectra change radically with more peaks being visible as the intershell multiple scattering pathlengths vary.

Spectra produced for structures where the carbonyl bond length was held constant while the Mo–C distance was changed by 0.2-Å shifts are shown in Figure 4. Increasing the pathlength of all scattering paths along this series leads to an oscillation with a higher frequency. The relative intensities of the three peaks are also affected, with the third peak becoming much stronger in the models with short Mo–C distances.

The effect of a tetragonal distortion to the hexacarbonyl species was also studied. If a 0.1-Å distortion to the Mo–C distance is applied little effect on the spectra is seen but when a larger 0.2-Å distortion is applied some changes are visible, notably a decrease in the separation of the first two maxima for the elongation and an increase in this distance for a contraction.

For the $Mo(CO)_4$ structure two configurations, tetrahedral and square planar, were considered, while five isomers of $Mo(CO)_5$, trigonal bipyramidal and four different square pyramidal forms, were examined. In all these cases the intershell distances used were those crystallogrpahically determined from $Mo(CO)_6$. Thus intrashell multiple scattering is responsible for any changes that are seen. The square-planar structure has the same pathways available as in the octahedral hexacarbonyl, hence it is not surprising that their calculated XANES spectra are similar (Figure 5). However, the tetrahedral structure gives a very different spectrum, which is similar to that for the $Mo(CO)_5$ square pyramid with a basal angle of 105° (Figure 6), which is close to the tetrahedral angle of 109.57°. For the trigonal bipyramid, with six 90°, three 120°, and one 180° bond angles, many of the intrashell paths are similar to those in $Mo(CO)_6$. Hence the

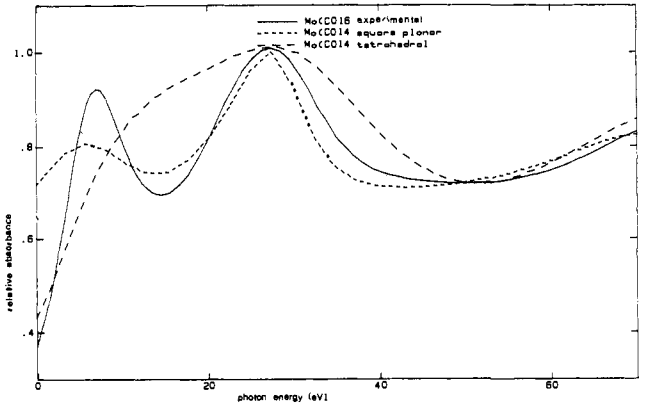

Figure 5. Theoretical XANES of $Mo(CO)_4$ species.

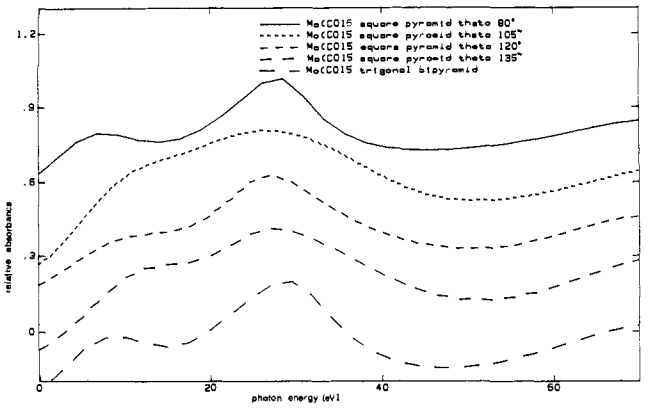

Figure 6. Theoretical XANES of $Mo(CO)_5$ species.

spectral likeness is predictable. This is even more so for the square pyramid with a 90° basal angle which is just $Mo(CO)_6$ with a ligand removed. As the basal angle is increased from 90° the first maxima diminishes and becomes a shoulder on the second. Then past 105° the two peaks begin to separate again. The separation of the second and third maxima is not altered much, indicating that further than about 50 eV from the edge the spectrum is affected little by this type of geometrical change. In summary, the $Mo(CO)_x$ XANES shows both geometrical and distance effects, though the former are only pronounced in the early part of the region where both types of multiple scattering can occur.

Mo–Mo Dimers. For the $[Mo_2Me_8]^{4-}$ anion the structural parameters from the crystal structure of the thf adduct[15] were used for the calculated model (Mo–Mo 2.15 Å, Mo–C 2.29 Å, Mo···Li 2.74 Å, Mo···C 3.54 Å). The four-shell fit includes four lithium atoms staggered with respect to the methyl groups around the midpoint of the Mo–Mo bond. Removing the carbon shell due to the methyl attached to the adjacent molybdenum atom appears to make little difference to the calculated XANES (Figure 7), but on close examination the two minima in the first derivative's spectrum coalesce when this shell is removed. Here in the XANES region shells not seen in EXAFS analysis have an effect. This may be due to the longer mean free path of electrons with energies of less than 15 eV.[16] Removing the lithium shell principally alters the relative amplitude of the first two peaks.

Increasing the molybdenum–carbon bond length by 0.2 Å causes the first peak to narrow as the separation of the first two maxima decreases, while a decrease in this bond length flattens the XANES spectrum as the main maxima separate. A change in the molybdenum–molybdenum bond length has less effect on the calculated spectra, though both an increase and a decrease slightly reduce the energy separation of the absorption maxima and narrow the first peak.

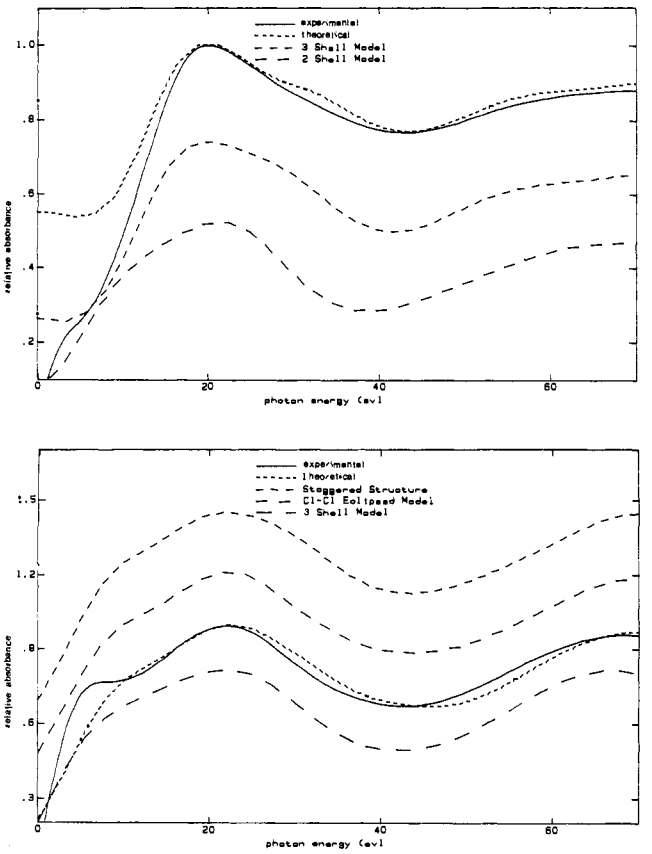

Figure 7. Experimental and theoretical XANES of $Li_4[Mo_2Me_8]$ (top) and $Mo_2Cl_4[P(n\text{-}Bu)_3]_4$ (bottom).

The shoulder on the white line is still apparent in all of the spectra and does not alter position much in any of them; it is, however, further from the top of the white line with a closer carbon shell. Thus the XANES is dominated by the low Z backscatterers rather than the molybdenum–molybdenum bond.

For $Mo_2Cl_4[P(n\text{-}Bu)_3]_4$ bond distances from the best-fit of the EXAFS spectrum and bond angles from the crystal structure of $Mo_2Cl_4[P(Me)_3]_4$[17] were used (Mo–Mo 2.14 Å, Mo–Cl 2.41 Å, Mo–P 2.58 Å, Mo···P 3.68 Å, Mo···Cl 3.78 Å). The fit between experimental and theoretical curves is quite good (Figure 7) though the two main maxima are slightly closer in the theoretical spectrum and the shoulder in the theoretical spectrum is not nearly as pronounced in the real XANES. The removal of the fourth and fifth shells produces little change in the calculated spectrum, although the shoulder on the white line is marginally flattened. Similarly changing the configuration of the cluster so the chlorine atoms eclipse each other has almost no effect. Introducing a staggered configuration increases the shoulder on the white line. These configurational changes only affect long type II multiple scattering paths and thus only are likely to alter the near XANES region of the spectrum.

Varying the molybdenum–ligand distances by 0.2 Å in each direction causes the anticipated effects one might expect: the longer bond lengths produce a shorter separation of the first two maxima, while for the shorter bonds lengths the opposite occurs as the peaks shift further apart. A 0.2-Å change in the metal–metal bond length in either direction causes a slight decrease in the energy difference of the two main features; this is similar to the effect this alteration had on the octamethyldimolybdenum(II) spectra.

For β-$Mo_2Cl_4(dppe)_2$ (dppe = bis(diphenylphosphino)ethane) and $Mo_2Cl_4py_4$ bond distances and bond angles from the crystal structure of β-$Mo_2Cl_4(dppe)_2$[18] and the EXAFS-determined bond

(15) Cotton, F. A.; Troup, J. M.; Webb, T. R.; Williamson, D. H.; Wilkinson, G. *J. Am. Chem. Soc.* **1974**, *96*, 3824.
(16) Teo, B. K. In *EXAFS: Basic Principles and Data Analysis*; Springer-Verlag: Berlin, 1986; pp 89–93.
(17) Cotton, F. A.; Extine, M. W.; Felthouse, T. R.; Kolthammer, B. W. S.; Lay, D. G. *J. Am. Chem. Soc.* **1981**, *103*, 4040.
(18) Agaskar, P. A.; Cotton, F. A. *Inorg. Chem.* **1984**, *23*, 3383.

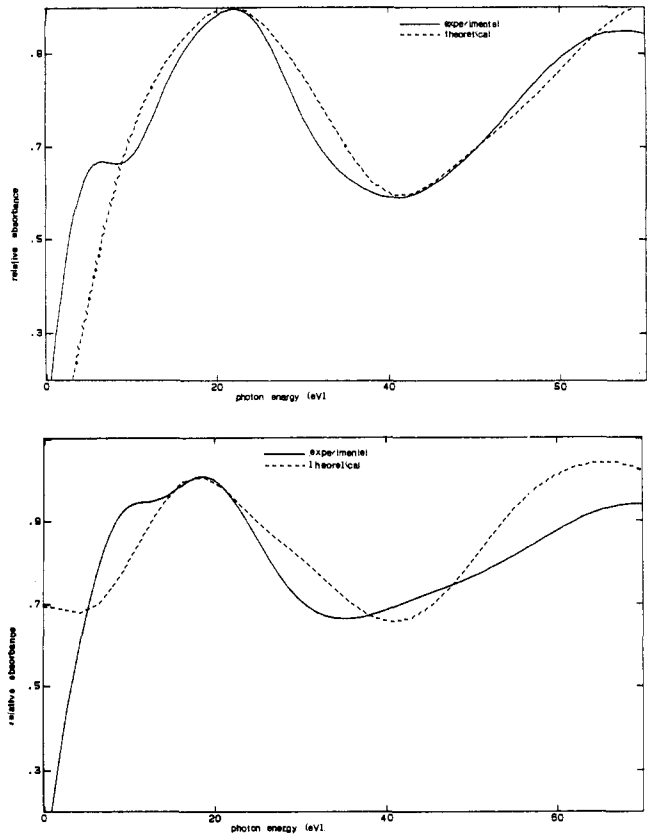

Figure 8. Experimental and theoretical XANES of β-$Mo_2Cl_4(dppe)_2$ (top) and $Mo_2Cl_4py_4$ (bottom).

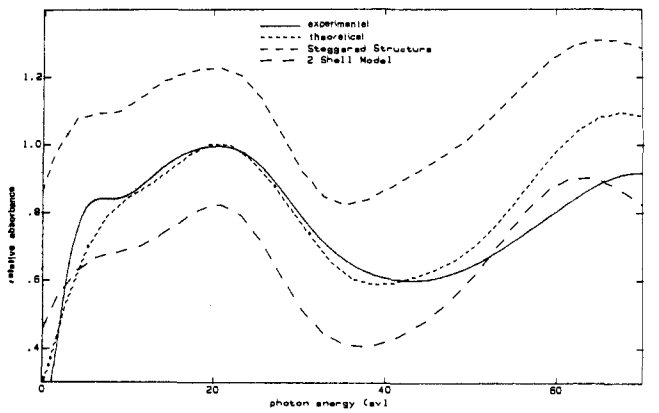

Figure 9. Experimental and theoretical XANES of the $[Mo_2Cl_8]^{4-}$ ion showing the effect of using fewer shells in the theoretical model.

distances of $Mo_2Cl_4py_4$ and bond angles from the crystal structure of the analogous $Mo_2Cl_4(4Me\text{-}py)_4$[19] were used to calculate the XANES of the two complexes. There is some agreement between the theoretical and experimental spectra in both cases (Figure 8), but the shoulders on the white lines are not well-defined in the calculated spectra. Moreover the separation of the two maxima is different for the calculated and experimental spectra in both cases, though the phosphine-calculated XANES matches the experimental XANES better than in the pyridine case.

For the $[Mo_2Cl_8]^{4-}$ ion both radial and geometric changes were made to see how they affected the calculated XANES spectra. Parameters from the crystal structure of the ammonium salt of the complex were used[20] (Mo–Mo 2.14 Å, Mo–Cl 2.44 Å, Mo···Cl 3.64 Å). There is good agreement between the spectra (Figure 9), though the separation of the two chief maxima is smaller in

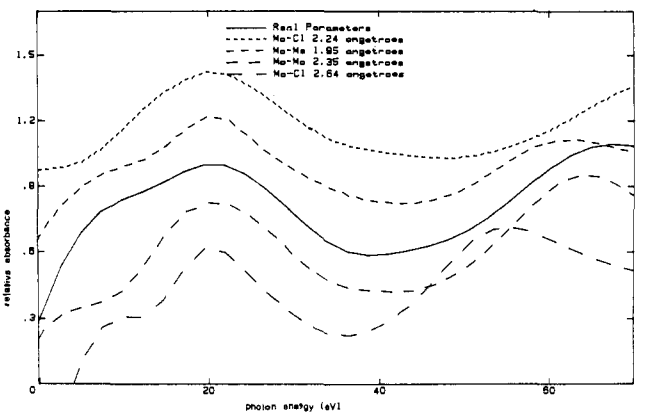

Figure 10. Theoretical XANES of the $[Mo_2Cl_8]^{4-}$ ion showing the effects of altering the Mo–Cl and Mo–Mo distances.

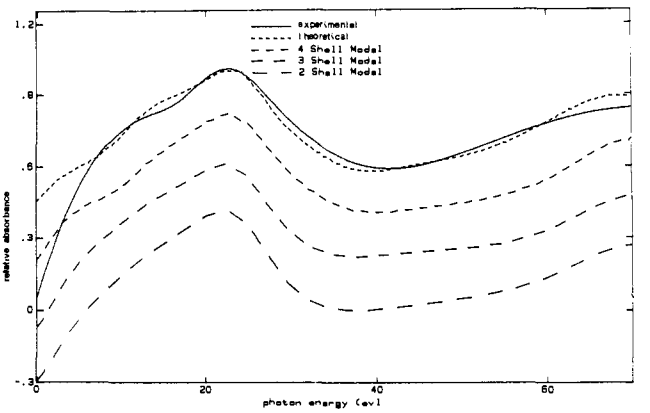

Figure 11. Experimental and theoretical XANES of $Mo_2(O_2CCH_3)_4$ showing the effect of using fewer shells in the theoretical model.

the calculated XANES and the intensity ratio of the two peaks differs and the shoulder on the first peak is better defined in the real XANES. Removing the second chlorine shell and giving the ion a staggered configuration do not alter the basic form of the calculated XANES. However the shoulder of the first peak is more clearly defined in both these spectra, perhaps indicating that here the third shell has little effect on the real XANES. Alterations to the Mo–Cl and the Mo–Mo bond lengths by 0.2 Å affect the spectrum to a much greater extent (Figure 10). The effect of a change in the Mo–Mo distance is to narrow the first peak making the shoulder more obvious. While the intensity ratio of two main features is altered substantially, their separation varies little throughout the three spectra. Changing the Mo–Cl distance affects both the shape of the first peak and the separation of the two maxima, with a longer bond producing a shorter separation as expected and vice versa. The distance between the position of the shoulder and the top of the main peak varies in the same fashion.

For $Mo_2(O_2CCH_3)_4$ the effect of the individual shells as well as changes in the shell radii were studied. The nonbonded oxygen atom at 2.64 Å from the molybdenum atom in the vacant octahedral site was included in the cluster. The parameters used were those found by X-ray crystallographic study[21] (Mo–Mo 2.09 Å, Mo–O 2.12 Å, Mo···O 2.64 Å, Mo···C 2.93 Å, Mo···O 3.02 Å). Once again the calculated and experimental spectra are very similar (Figure 11); the chief differences are the intensity ratio of the two peaks and the relative prominence of the shoulder on the first peak. The difference between the two-shell calculated XANES and the five-shell calculated XANES is not large. It principally concerns the shape and position of the shoulder on the first maxima. This bears the closest resemblance to the experimental XANES for the five-shell model, with the shoulder being

(19) Brencic, J. V.; Golic, L.; Leban, I.; Segedin, P. *Monatsh. Chem.* **1979**, *110*, 1221.
(20) Brencic, J. V.; Cotton, F. A. *Inorg. Chem.* **1970**, *9*, 346.
(21) Cotton, F. A.; Mester, Z. C.; Webb, T. R. *Acta Crystallogr., Sect. B* **1974**, *30*, 2768.

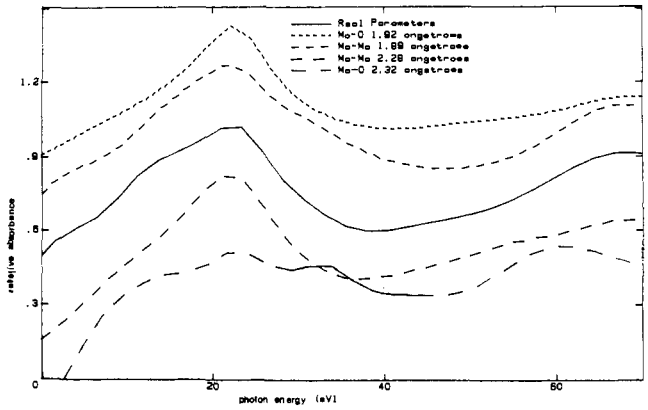

Figure 12. Theoretical XANES of $Mo_2(O_2CCH_3)_4$ showing the effect of altering the Mo–O, Mo–C, and Mo–Mo distances.

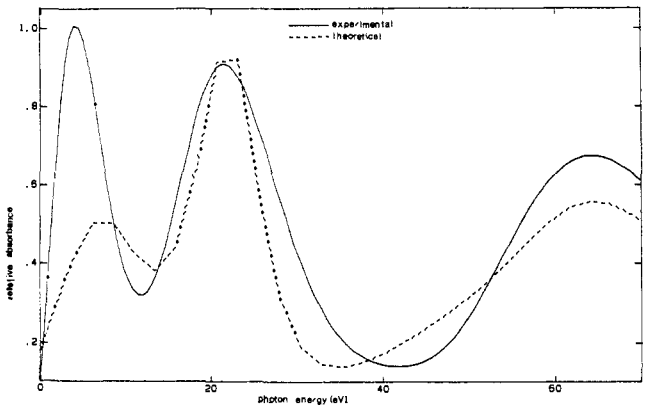

Figure 13. Experimental and theoretical XANES of the $[Mo(CN)_8]^{4-}$ ion.

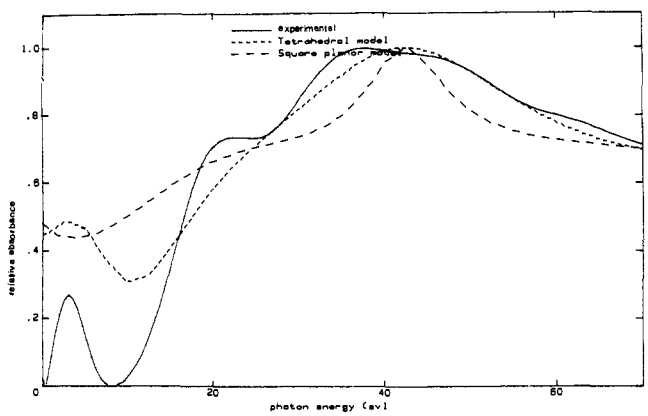

Figure 14. Experimental and theoretical XANES of the $[MoO_4]^{2-}$ ion with both a square-planar and a tetrahedral model.

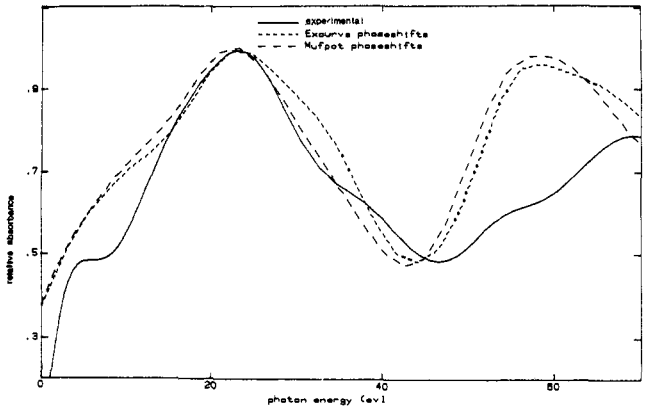

Figure 15. Experimental and theoretical XANES of MoS_2 with both EXCURVE and MUFFPOT/PSM calculated phase shifts.

less prominent and the main minima being much flatter in the other spectra. Changing the metal–metal distance makes very little difference to the calculated spectra (Figure 12), again showing that low Z atoms affect the XANES region of the absorption spectrum much more than high Z atoms. For the changes in shell radii the Mo–C shell radius was altered so that the distance from the carbon atoms to the molybdenum–molybdenum axis was constant when the metal–metal distance was varied and was changed by the same amount as the first oxygen shell radius when the latter was altered. Changing the metal–ligand distances makes a large difference to the calculated XANES. These changes can be summarized as the shorter shell radii producing almost a one-peak spectrum, as the second peak gets much flatter, and the longer metal–ligand distances giving rise to broader peaks which are closer to each other.

Other Molybdenum Compounds. By using crystallographically-derived parameters[22] a reasonable similarity with regard to peak position was achieved for $K_4[Mo(CN)_8]\cdot 2H_2O$ (Figure 13).

$[MoO_4]^{2-}$ is a simple one shell species[23] and hence is a suitable subject for the study of the effect of molecular geometry on calculated XANES. The square-planar structure gives rise to a spectrum (Figure 14), with a narrow first peak with a shoulder, that is dissimilar to the tetrahedral calculated spectrum. The latter, while it does not have the shoulder, matches both the width of the main maxima of the real structure and the pre-edge peak much better. Changing the molybdenum–oxygen distance principally alters the separation of the pre-edge peak and also the separation of the two peaks in the main maxima.

For molybdenum disulfide two approaches were made. In addition to the method of using EXCURVE-calculated phase shifts in the DLXANES program, an attempt to calculate more accurate phase shifts was made. This involved using charge densities calculated by the program PINKPANTHER[24] in the program MUFFPOT[25] with the real structural parameters[26] using 7 shells out to a 6-Å radius to calculate the muffin-tin potentials and then using the program PSM[27] to compute phase shifts from those potentials. The muffin-tin potentials used are constructed by the "Mattheiss prescription".[28]

For the neutral atom charge densities are constructed by some Herman–Skillman-like self-consistent-field atomic calculations. These charge densities are put into each site of the atomic geometry, and the superposed potential is spherically averaged around the atom of interest. Then this charge density is used in solving the Poisson equation for the Coulomb part of the potential, while the exchange-correlation potential is found by means of a local approximation, using an $X\alpha$-type formula with $\alpha = 1$. The justification for this is heuristic,[29] and moreover it may be that geometry is more important then the potentials in XANES.

The simple method bears some similarity to the experimental spectrum, though the separation of the two main maxima is smaller than in the observed spectrum (Figure 15). Unfortunately this difference was not remedied by the more thorough attempt, though different muffin-tin radii were tried in attempts to mimic the experimental XANES. Full band structure calculations may solve this problem as a recent study of MoS_2 by Binsted shows.[30]

A major problem with this theoretical approach concerns the generalized potentials used. This is probably the main cause of

(22) Hoard, J. C.; Hamer, T. A.; Glick, M. D. *J. Am. Chem. Soc.* **1968**, *90*, 3177.
(23) Gatehouse, B. M.; Leverett, P. *J. Chem. Soc. A* **1969**, 849.
(24) Desclaux, J. P. PINKPANTHER program modified by Durham, P. J.
(25) Durham, P. J. S.E.R.C. Daresbury Laboratory MUFFPOT program, 1987.
(26) Takeuchi, Y.; Nowacki, W. *Schweiz. Mineral. Petrogr. Mitt.* **1964**, *44*, 105.
(27) Durham, P. J. S.E.R.C. Daresbury Laboratory PSM program, 1987.
(28) Mattheiss, L. *Phys. Rev. A* **1964**, *134*, 970.
(29) Durham, P. J. In *EXAFS and Near-Edge Structure*; Bianconi, A., Incoccia, L.; Stipcich, S. Eds.; Springer Verlag: Berlin, 1983; pp 37–42.
(30) Binsted, N. Unpublished results.

disagreement between the observed and the calculated XANES spectra. In the near-XANES region the disagreements are worse for molybdenum joined to the second-row elements than to the first-row elements, and thus calculated XANES for carbon and oxygen systems may be more useful than for chlorine and phosphorus ones. Very close to the edge there are also many-body effects which a single potential may fail to represent. Background subtraction in the XANES region is difficult, thus it is unlikely this difficulty can be overcome with use of experimental phase shifts.

The restriction imposed on the maximum value of 3 for angular momentum, *l*, used means the final part of the calculated spectrum is not as reliable as the rest. For the dimers the metal–ligand distance is the dominant factor in determining the shape of the XANES though the metal–metal interaction does also affect the spectra.

Electronic band structure calculation methods for XANES are not a viable option for most structures, especially the unknown ones. Even when these can be done they have two major problems:[31] first, they provide a high degree of detail which is washed out by various broadenings and lifetime effects; second, it is difficult to include other important physical constraints such as core-hole potentials and final-state lifetime effects in anything but an ad hoc manner. Since the electronic band structure approach has already summed all the scattering paths, specific path contributions and thus bond angle information can be difficult to extract.

The limitations in this approach to XANES calculations are obvious from this study but some geometrical conclusions seem possible, as does the detection of other shells, not discernible in EXAFS, particularly those of low Z elements. The effect of type II multiple scattering, which provides this information, is seen in the early part of the XANES region but sometimes e.g. in $[MoO_4]^{2-}$ rather further out than the 13-eV limit suggested by Stern and Bunker.[2] Excellent fits as achieved in EXAFS analyses are not achievable at present, but routine XANES analyses combined with the former can tell which structures are most likely and which are not.

Experimental Section

Reagent grade $Mo(CO)_6$ and MoS_2 were purchased from the Aldrich Chemical Co. $K_4Mo(CN)_8 \cdot 2H_2O$,[32] $Na_2MoO_4 \cdot H_2O$,[23] $(NH_4)_3Mo_2Cl_9 \cdot H_2O$,[34] $Mo_2Cl_4py_4$,[35] β-$Mo_2Cl_4(dppe)_2$,[36] $Li_4Mo_2(Me)_8 \cdot 4Et_2O$,[15] and $Mo_2(AcO)_4$[37] were all made by standard literature methods, while $Mo_2Cl_4[P(n\text{-}Bu)_3]_4$ was made following the route of Glicksman et al.[38] for $Mo_2Cl_4(PEt_3)_4$.

All spectra were recorded in transmission at room temperature on station 9.2 of the S.R.S., S.E.R.C. Daresbury Laboratory with an order-sorting Si(220) monochromator detuned by 50% for harmonic rejection. The samples were diluted to 10 wt % Mo by dry boron nitride and held between "Sellotape" in a 3 mm thick aluminium sample holder. The $Mo_2Cl_4[P(n\text{-}Bu)_3]_4$, $Li_4Mo_2(Me)_8 \cdot 4Et_2O$, and $Mo_2(AcO)_4$ samples were prepared in a dry nitrogen glovebox.

Theoretical spectra were calculated with the program DLXANES on a Convex C-220 computer. Several inelastic effects are modeled by a constant imaginary potential, which in principle should be energy dependent;[39] for the real structures this was varied in the range -2 to -4 eV to give the best fit between the experimental and theoretical curves. For the theoretical structures the same value as that employed in the comparable real structure was used. With one exception, discussed above, the phase shifts and the molybdenum matrix elements used were those calculated ab initio in EXCURVE.[40] These are the same phase shifts as those used in EXAFS data analysis. They are independent of the environment of atom and thus cannot be expected to be a perfect representation for every case. But they have the advantage that nothing need be known about the structure of the system before the calculation is performed. More accurate potentials leading to more accurate phase shifts should lead to better results if the error introduced by the inaccuracies in the phase shifts is significant in terms of other errors arising from many-body effects.

The principal requirement for obtaining good XANES spectra is high-energy resolution. This effectively means that only a small part of the vertical component of the beam can be used, with consequent loss of beam intensity. For EXAFS a resolution of about 10 eV is reasonable, but XANES requires higher resolution. The vertical beam height of ca. 0.5 mm used gives a resolution of ca. 3 eV on this station. Hence it is likely some features are blurred in the experimental spectra, though since the natural line width of the Mo K-edge is 4.2 eV,[41] there is a certain amount of natural broadening.

Acknowledgment. We are grateful to the S.E.R.C. for financial support, a studentship (J.F.W.M.), and the use of the facilities of the S.R.S., whose staff we would like to thank for their help with our experiments. We acknowledge N. Binsted for useful discussions. We thank Dr. J. T. Gauntlett for help in recording the spectra.

(31) Albers, R. C. *Physica B* **1989**, *158*, 372.
(32) Van de Poel, J.; Newmann, H. W. *Inorg. Synth.* **1968**, *9*, 53.
(33) Reference deleted in proof.
(34) Brencic, J. V.; Cotton, F. A. *Inorg. Chem.* **1970**, *9*, 351.
(35) San Filippo, J., Jr.; Sniadoch, H. J.; Grayson, R. L. *Inorg. Chem.* **1974**, *13*, 9.
(36) Cole, N. F.; Derringer, D. R.; Fiore, E. A.; Knoechel, D. J.; Schmitt, R. K.; Smith, T. J. *Inorg. Chem.* **1985**, *24*, 1978.
(37) Brignole, A. B.; Cotton, F. A. *Inorg. Synth.* **1972**, *13*, 88.
(38) Glicksman, H. D.; Hamer, A. D.; Smith, T. J.; Walton, R. A. *Inorg. Chem.* **1976**, *15*, 2204.
(39) Gurman, S. J. *J. Phys. C* **1983**, *16*, 2987.
(40) Binsted, N.; Gurman, S. J.; Campbell, J. W. S.E.R.C. Daresbury Laboratory EXCURVE program, 1984.
(41) Krause, M. O.; Oliver, J. H. *J. Chem. Phys. Ref. Data* **1979**, *8*, 329.